

Activation of the transcription factor EB rescues lysosomal abnormalities in cystinotic kidney cells



Laura R. Rega¹, Elena Polishchuk², Sandro Montefusco², Gennaro Napolitano², Giulia Tozzi³, Jinzhong Zhang⁴, Francesco Bellomo¹, Anna Taranta¹, Anna Pastore⁵, Roman Polishchuk², Fiorella Piemonte³, Diego L. Medina², Sergio D. Catz⁴, Andrea Ballabio² and Francesco Emma¹

¹Division of Nephrology and Dialysis, Bambino Gesù Children's Hospital and Research Institute, Rome, Italy; ²Telethon Institute of Genetics and Medicine, Pozzuoli (Naples), Italy; ³Unit for Muscular and Neurodegenerative Diseases, Bambino Gesù Children's Hospital and Research Institute, Rome, Italy; ⁴Department of Molecular and Experimental Medicine, The Scripps Research Institute, La Jolla, California, USA; and ⁵Laboratory of Proteomics and Metabolomics, Bambino Gesù Children's Hospital and Research Institute, Rome, Italy

Nephropathic cystinosis is a rare autosomal recessive lysosomal storage disease characterized by accumulation of cystine into lysosomes secondary to mutations in the cystine lysosomal transporter, cystinosin. The defect initially causes proximal tubular dysfunction (Fanconi syndrome) which in time progresses to end-stage renal disease. Cystinotic patients treated with the cystine-depleting agent, cysteamine, have improved life expectancy, delayed progression to chronic renal failure, but persistence of Fanconi syndrome. Here, we have investigated the role of the transcription factor EB (TFEB), a master regulator of the autophagy-lysosomal pathway, in conditionally immortalized proximal tubular epithelial cells derived from the urine of a healthy volunteer or a cystinotic patient. Lack of cystinosin reduced TFEB expression and induced TFEB nuclear translocation. Stimulation of endogenous TFEB activity by genistein, or overexpression of exogenous TFEB lowered cystine levels within 24 hours in cystinotic cells. Overexpression of TFEB also stimulated delayed endocytic cargo processing within 24 hours. Rescue of other abnormalities of the lysosomal compartment was observed but required prolonged expression of TFEB. These abnormalities could not be corrected with cysteamine. Thus, these data show that the consequences of cystinosin deficiency are not restricted to cystine accumulation and support the role of TFEB as a therapeutic target for the treatment of lysosomal storage diseases, in particular of cystinosis.

Kidney International (2016) **89**, 862–873; <http://dx.doi.org/10.1016/j.kint.2015.12.045>

KEYWORDS: cystinosis; pediatric nephrology; proximal tubule; renal pathology

© 2016 International Society of Nephrology

Cystinosis is a rare autosomal recessive lysosomal storage disease (LSD) with an incidence of 0.5 to 1.0 per 100,000 live births. The most severe and frequent form, affecting ~95% of patients, is the infantile nephropathic cystinosis (OMIM 219800).¹ All clinical forms of cystinosis are caused by bi-allelic mutations in the *CTNS* gene, which is located on chromosome 17p13. More than 100 mutations have been reported;² however, the most frequent mutation, found in northern European patients, is a large deletion of 57,257 base pairs, involving the first 9 *CTNS* exons and part of exon 10.³ The *CTNS* gene encodes the lysosomal cystine transporter, cystinosin, which is a 367 amino acid lysosomal protein that contains 7 transmembrane domains.⁴ Cystinosin is a proton-cystine symporter devoted to the excretion of both cystine and protons out of the lysosomal lumen.⁵ Because cystinosin is ubiquitously expressed, its absence or malfunctioning causes accumulation of cystine into the lysosomes throughout the body. Moreover, cystine is poorly soluble, thus its accumulation leads to the formation of crystals. Kidneys are one of the first organs to be affected in cystinotic patients, which typically present with clinical signs of Fanconi syndrome, by 4 to 6 months of age. Fanconi syndrome is characterized by polyuria and abnormal urinary loss of amino acids, glucose, low-molecular-weight and intermediate-weight proteins, and other solutes. If untreated, patients progress to end-stage renal disease by the age of 10 years.⁶ The mechanisms linking lysosomal cystine accumulation to cell dysfunctions, in particular to the prominent proximal tubular defect, remain unclear. Recent studies have generated various hypotheses indicating that proximal tubule damage is associated with increased sensitivity to apoptosis,^{7,8} abnormal autophagy,^{9,10} mitochondrial dysfunction,¹¹ adenosine triphosphate depletion,¹¹ increased reactive oxygen species production,¹¹ endoplasmic reticulum stress,¹² endo-lysosomal dysfunctions,¹³ and cell dedifferentiation.^{14,15}

Cysteamine was introduced in the late 1970s for the treatment of cystinosis and has been the only therapy available since then.^{16,17} However, foul odor and gastric side effects of oral cysteamine make adherence extremely difficult. Moreover, cysteamine does not correct all the symptoms of cystinosis; in particular, it does not have an impact on the renal Fanconi syndrome.¹ Even well-treated patients will

Correspondence: L.R. Rega, Division of Nephrology and Dialysis, Bambino Gesù Children's Hospital, Piazza Sant'Onofrio, 4, 00165 Rome, Italy. E-mail: laurarita.rega@opbg.net

Received 11 May 2015; revised 22 December 2015; accepted 30 December 2015

eventually progress to envisage renal disease and will require kidney transplantation. Thus, novel therapeutic approaches are needed for cystinosis.

The recent discovery of a lysosomal gene network, the coordinated lysosomal expression and regulation network and of its master regulator, transcription factor EB (TFEB), has provided new insights in the studies of LSD.¹⁸ TFEB activates the transcription of genes that encode lysosomal proteins involved in several aspects of cellular clearance, such as lysosomal biogenesis, exocytosis, and autophagy, as well as nonlysosomal proteins involved in the degradation of autophagy substrates.¹⁹ The role of TFEB in promoting cellular clearance has been proven in several diseases such as multiple sulfatase deficiency,²⁰ Pompe disease,²¹ and alpha-1-anti-trypsin deficiency.²² Together these findings provide proof of concepts that drugs that stimulate TFEB activity may represent useful therapeutic tools to enhance mobilization of aberrant storage materials in LSD.

Herein, we have investigated the impact of TFEB activation on 3 cystinotic phenotypes, namely lysosomal cystine accumulation, delayed processing of endocytic cargo and aberrant lysosomal compartment morphology. We have observed that cystinosis-depleted cells have reduced expression of TFEB. Moreover, abnormalities of the lysosomal compartment induced by cystinosis deficiency are associated with TFEB nuclear translocation. Both chemical and genetic stimulation of TFEB activity promotes clearance of cystine storages within 24 hours. Overexpression of TFEB stimulates also delayed cargo processing. Prolonged increased expression of TFEB could also rescue other defects of the lysosomal compartment in cystinotic cells that are not sensitive to cysteamine. These results support the role of TFEB as a therapeutic target for the treatment of LSDs and provide promising perspectives in the treatment of cystinosis.

RESULTS

CTNS-depleted cells have reduced TFEB expression

Endogenous expression of TFEB was analyzed in conditionally immortalized proximal tubular epithelial cells (ciPTEC) derived from the urine of a healthy volunteer or a cystinotic patient bearing the homozygous 57-kb deletion of the *CTNS* gene. Immunoblotting experiments performed on total cell extracts revealed reduced levels of endogenous TFEB in *CTNS*^{-/-} ciPTEC, compared with *CTNS*^{+/+} ciPTEC (~40%) (Figure 1a). Quantitative real-time polymerase chain reaction (PCR) also showed similar reduction of TFEB mRNA levels in *CTNS*^{-/-} ciPTEC (~40%) (Figure 1b). Depleting intracellular cystine in *CTNS*^{-/-} ciPTEC by cysteamine treatments did not rescue the defect of expression of TFEB (Figure 1b). Cysteamine treatment produced ~90% reduction of total cystine levels in *CTNS*^{-/-} ciPTEC (Supplementary Figure S1A).

To prove that this effect was not specific of this cell line, we confirmed these results with a RNA interference approach. To this end, human kidney-2 cells were transfected with nontargeting (CTRL) or *CTNS* short interfering RNAs (*CTNS* knock down) and analyzed for TFEB expression. Immunoblotting

experiments showed reduction of TFEB in *CTNS* knocked down cells (~50%) (Figure 1c). Quantitative real-time PCR also revealed ~40% reduction of TFEB mRNA levels in human kidney-2 cells silenced for *CTNS* expression (Figure 1d). The efficiency of *CTNS* silencing was approximately 60% in human kidney-2 cells (Figure 1e). Reduction of TFEB mRNA was also shown in HepG2 cells silenced for *CTNS* expression (Supplementary Figure S1B and C).

Together these results indicate that lack of cystinosis impairs TFEB expression.

TFEB is translocated into the nucleus of cystinotic cells

To address TFEB intracellular distribution, we performed nuclear-cytoplasmic fractionation experiments. Immunoblotting experiments revealed increased nuclear-cytoplasmic ratio of TFEB protein levels in cystinotic *CTNS*^{-/-} ciPTEC, compared with control *CTNS*^{+/+} ciPTEC (~3.5-fold increase), indicating increased nuclear translocation of TFEB in cystinotic cells (Figure 2a).

Control and cystinotic ciPTEC were also transiently transfected with a TFEB–green fluorescent protein (GFP) plasmid. After 24 hours, fluorescence analysis showed a 2-fold increase in TFEB–GFP nuclear translocation in *CTNS*^{-/-} ciPTEC, as compared to control *CTNS*^{+/+} cells (Figure 2b).

TFEB activation promotes reduction of cystine stores in cystinotic cells

To stimulate activation of endogenous TFEB, cystinotic *CTNS*^{-/-} ciPTEC were treated with genistein (100 μM) for 24 hours.²³ As expected, upon genistein treatment, cystinotic ciPTEC showed increased mRNA levels of representative coordinated lysosomal expression and regulation network genes, indicating genistein-mediated TFEB activation (~5-fold increase of *SQSTM1*, ~3-fold increase of both *ASAH1* and *CTSD*, ~1.6-fold increase in *SMPD1*) (Supplementary Figure S1D). Next, we checked the impact of genistein treatment on intracellular cystine levels. After genistein treatment, cystinotic ciPTEC showed ~40% reduction of cystine levels compared with vehicle (dimethyl sulfoxide [DMSO])–treated cells (Figure 3a). These data were also confirmed in fibroblasts obtained from a cystinotic patient bearing a heterozygous mutation in *CTNS* gene (c.18-21del.GATC c.255+3 A>T mutation) (~40% reduction of cystine levels in genistein-treated fibroblasts, as compared to DMSO-treated cells) (Supplementary Figure S1E).

In addition, we analyzed the effect of exogenous TFEB overexpression on cell cystine levels. *CTNS*^{-/-} ciPTEC were transduced with control GFP or TFEB–GFP lentiviral vectors. The GFP and TFEB–GFP transduced cells were sorted to 99% purity (data not shown) and cultured for 4 weeks. Overexpression of TFEB–GFP in cystinotic ciPTEC cells resulted in significant reduction (~60%) of total cystine levels, compared with cystinotic ciPTEC cells transduced with control GFP (Figure 3b). These data were further confirmed by transient transfection. After 24 hours, TFEB–GFP transfected

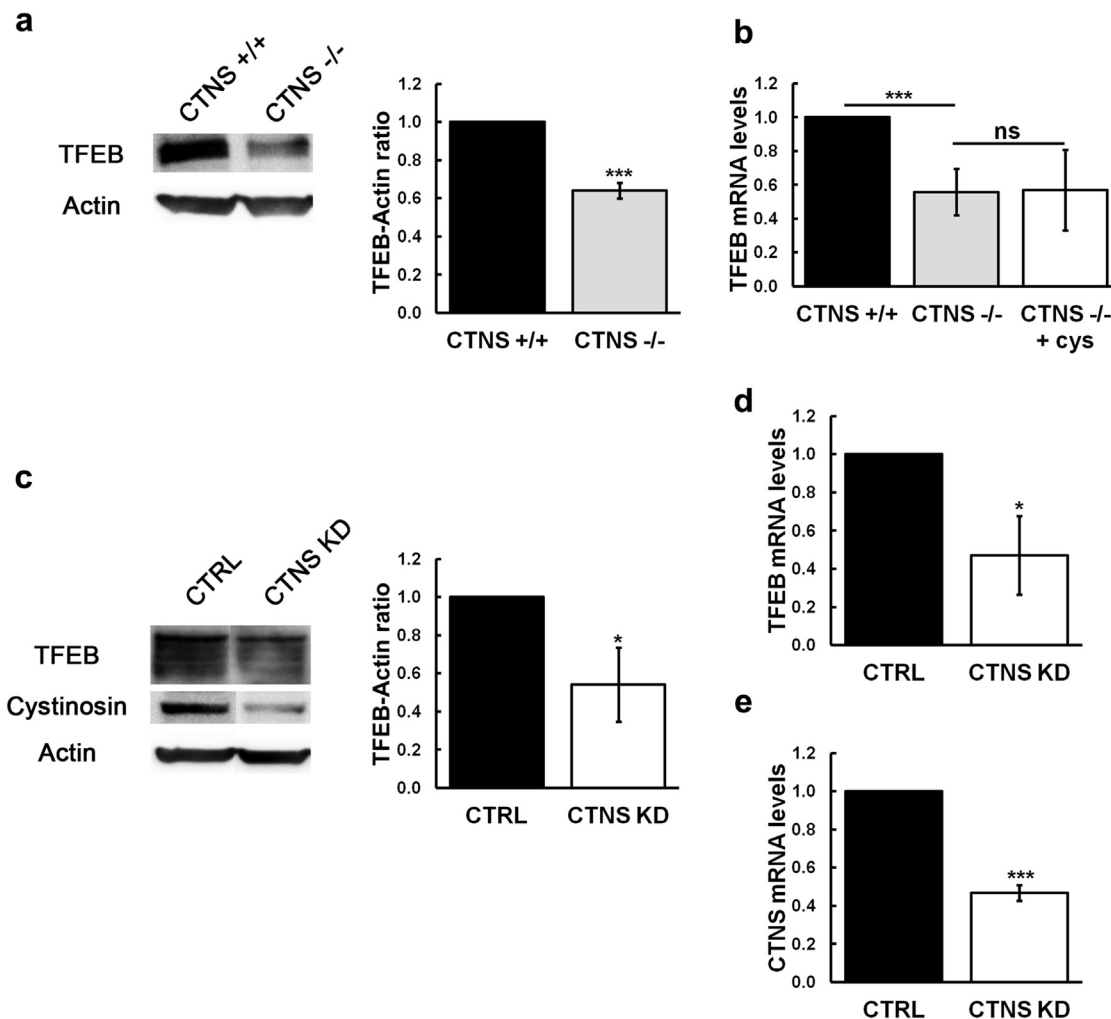


Figure 1 | CTNS depletion affects endogenous TFEB levels. (a) Representative immunoblot of transcription factor EB (TFEB) levels in total lysates from control *CTNS*^{+/+} and cystinotic *CTNS*^{-/-} conditionally immortalized proximal tubular epithelial cells. Results were normalized for Actin levels (loading control). The histogram shows TFEB-Actin mean ratios expressed as fold change \pm SD from 3 independent experiments, each in triplicate ($n = 3$; *** $P < 0.001$). (b) TFEB mRNA levels were analyzed in *CTNS*^{+/+}, *CTNS*^{-/-}, and conditionally immortalized proximal tubular epithelial cells untreated or treated with 100 μ M cysteamine (cys) for 24 hours by quantitative polymerase chain reaction, with glyceraldehyde-3-phosphate dehydrogenase used as reference. Data are presented as mean fold change \pm SD from 5 independent experiments, each in triplicate ($n = 5$; *** $P < 0.001$). (c) Representative immunoblots of TFEB, cystinosin, and actin levels in total cell lysates from human kidney-2 cells after 96 hours from transfection with nontargeting (CTRL) or CTNS small, interfering RNAs (CTNS knock down). The histogram shows the TFEB-actin mean ratio expressed as fold change \pm SD from 3 independent experiments ($n = 3$; * $P < 0.05$). (d) TFEB mRNA and (e) CTNS mRNA levels were analyzed in CTRL and CTNS knocked down human kidney-2 cells. Glyceraldehyde-3-phosphate dehydrogenase was used as reference. Data are presented as mean fold change \pm SD from 3 independent experiments, each in triplicate ($n = 3$; * $P < 0.05$; *** $P < 0.001$).

CTNS^{-/-} ciPTEC showed ~60% reduction of cystine levels, as compared to control GFP transfected cells (Figure 3c). Moreover, transfection of the constitutive active mutant TFEB(S142A)-GFP induced stronger reduction of cystine levels in *CTNS*^{-/-} ciPTEC, as compared to TFEB-GFP transfected cells (~80%) (Figure 3c).

To elucidate the mechanisms by which TFEB promotes clearance of cystine accumulation in cystinosis, we analyzed the activities of the lysosomal enzyme β -hexosaminidase. Significantly higher levels of lysosomal β -hexosaminidase activities were detected in the medium of cystinotic *CTNS*^{-/-} ciPTEC overexpressing TFEB-GFP, compared with cystinotic

ciPTEC overexpressing control GFP (~2-fold increase) (Figure 3d). Consistently, we also measured increased cystine levels in the medium of *CTNS*^{-/-} ciPTEC overexpressing TFEB-GFP, compared with *CTNS*^{-/-} ciPTEC overexpressing control GFP (~2-fold increase) (Figure 3e). These effects were not a consequence of loss of plasma membrane integrity because we measured no statistically significant differences in positivity to propidium iodide between control GFP and TFEB-GFP *CTNS*^{-/-} ciPTEC (Supplementary Figure S1F). All together, these data indicate that TFEB activation promotes clearance of cystine stores by increasing lysosomal exocytosis.

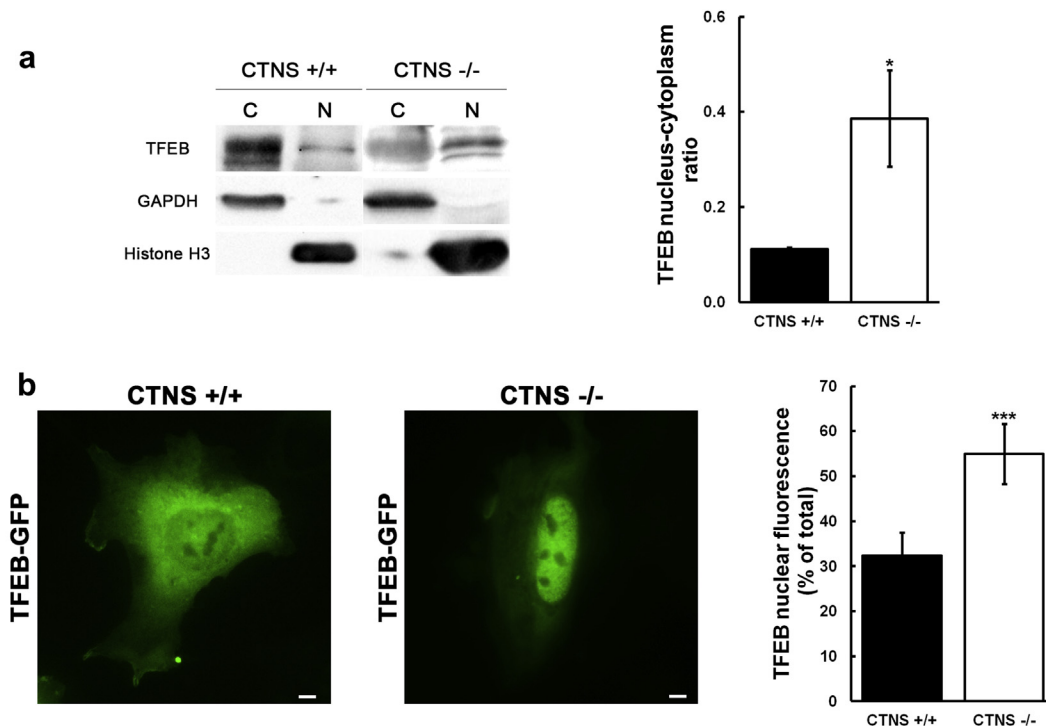


Figure 2 | TFEB nuclear translocation is increased in cystinotic cells. (a) Representative immunoblots showing transcription factor EB (TFEB) levels in both cytosolic (C) and nuclear (N) fractions from *CTNS*^{+/+} and *CTNS*^{-/-} conditionally immortalized proximal tubular epithelial cells. TFEB cytosolic and nuclear levels were normalized for glyceraldehyde-3-phosphate dehydrogenase (GAPDH) and histone H3 levels, respectively. The histogram shows TFEB nucleus-cytoplasm ratios expressed as mean \pm SD from 3 independent experiments, each in triplicate ($n = 3$; $*P < 0.05$). (b) *CTNS*^{+/+} and *CTNS*^{-/-} conditionally immortalized proximal tubular epithelial cells were transiently transfected with TFEB-green fluorescent protein (GFP) plasmid (green). Bar = 10 μ m. After 24 hours from transient transfection, TFEB nuclear fluorescence intensity was measured by ImageJ software and expressed as percentage of total fluorescence intensity (normalized for the areas). Data are shown as means \pm SD from 5 independent experiments, each in duplicate ($n = 5$; $***P < 0.001$). GFP, green fluorescent protein.

TFEB activation stimulates cargo processing in cystinotic cells

To study the impact of TFEB activation on cystinotic endocytosis dysfunction, we evaluated the impact of TFEB overexpression on receptor-associated protein (RAP)-glutathione-S-transferase (GST) cargo processing. First, we confirmed delayed cargo processing in cystinotic cells.¹³ To this end, *CTNS*^{+/+} and *CTNS*^{-/-} ciPTEC were preincubated with RAP-GST ligand and transferred to 37 °C to allow internalization of the ligand bound to the cell surface. At indicated time points, cells were fixed and stained for RAP-GST (Figure 4a). In *CTNS*^{-/-} ciPTEC, RAP-GST remained visible for significantly longer time (30 minutes) after internalization, in comparison to control cells (Figure 4a and b). Then, we analyzed RAP-GST cargo processing in *CTNS*^{-/-} ciPTEC transfected with TFEB-GFP. After 30 minutes from cargo internalization, RAP-GST structures showed significant reduced size in TFEB-GFP positive cells, if compared with those in adjacent nontransfected cells ($\sim 50\%$) (Figure 4c and d). No statistically significant differences in the size of RAP-GST structures were observed between untransfected or TFEB-GFP transfected *CTNS*^{-/-} ciPTEC after 15 and 45 minutes from the shift to 37 °C (Figure 4c and d). Moreover, no statistically significant differences in RAP-GST processing were highlighted between untransfected or control GFP transfected *CTNS*^{-/-} ciPTEC (data not shown).

These data confirm delayed cargo processing in cystinotic cells and show that TFEB overexpression is able to rescue this defect.

TFEB overexpression reduces the number and size of lysosomes in cystinotic cells

Based on the findings that TFEB promotes mobilization of cystine depositions and enhances lysosomal exocytosis in cystinotic cells, we wondered whether in these experimental conditions the structure of the lysosomal compartment was also modified. We first checked differences in the number and size of lysosomes between control and cystinotic cells by immuno-electron microscopy (EM). To this end, control and cystinotic ciPTEC cells were labeled with anti-LAMP1 antibody and prepared for ultrastructural analysis. Cystinotic ciPTEC cells showed increased number of LAMP1 positive structures, as compared to control cells (the mean number of LAMP1 positive structures/field was 6 ± 0.3 , in *CTNS*^{+/+} and 10 ± 0.9 , in *CTNS*^{-/-}) (Figure 5a, b, and e). Measurements of the diameter of these LAMP1 positive structures also revealed increased size of lysosomes in cystinotic cells (mean diameter of 421.8 ± 20.3 nm and 594.6 ± 23.4 nm, in control and cystinotic cells, respectively) (Figure 5f). We then analyzed cystinotic ciPTEC transduced with GFP or TFEB-GFP lentiviruses. After TFEB-GFP overexpression, the number and the size of LAMP1 positive structures in cystinotic cells was

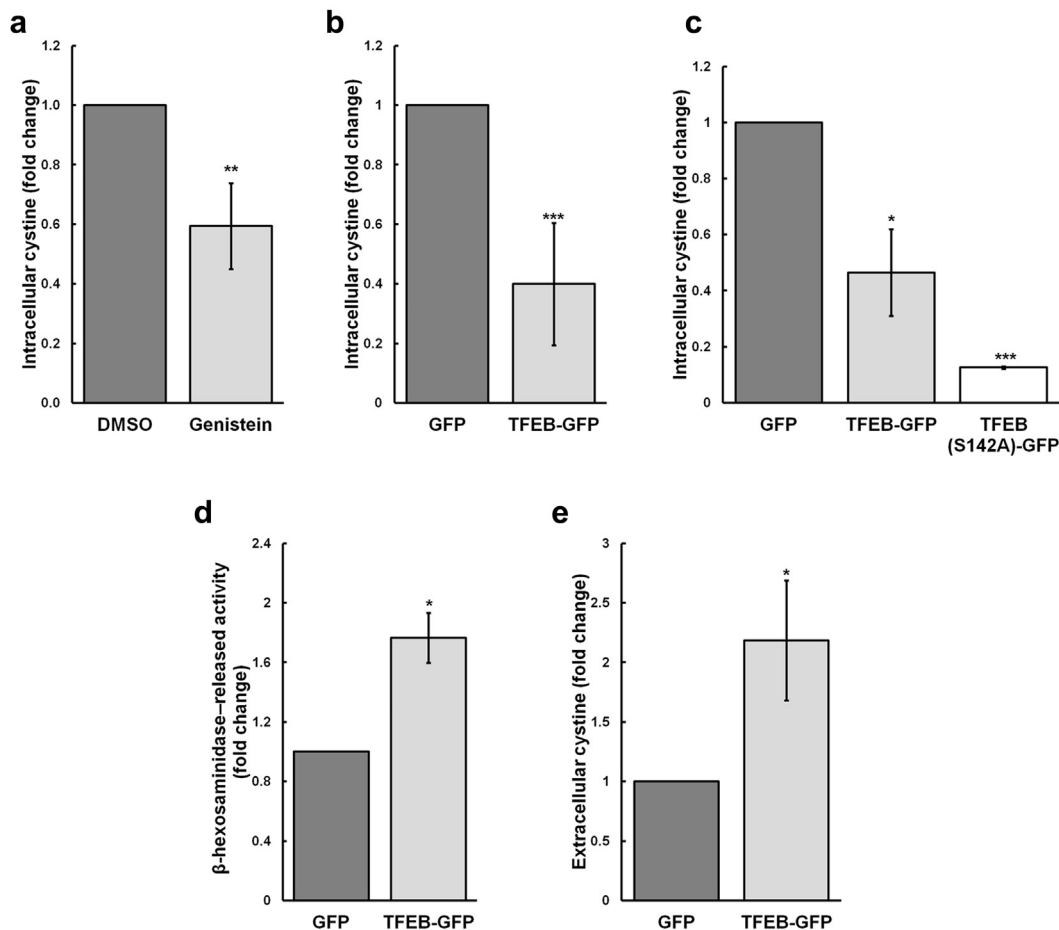


Figure 3 | TFEB promotes clearance of cystine from cystinotic cells. Intracellular cystine levels were measured in (a) *CTNS*^{-/-} conditionally immortalized proximal tubular epithelial cells (ciPTEC) after treatment with 100 μM genistein for 24 hours, corrected for protein concentrations, and normalized to those of dimethyl sulfoxide (DMSO)-treated cells. Data are presented as mean fold change ±SD from 3 independent experiments, each in triplicate (*n* = 3; ****P* < 0.01). (b) Intracellular cystine levels were measured in transcription factor EB (TFEB)-green fluorescent protein (GFP) transduced *CTNS*^{-/-} ciPTEC, as described herein, and normalized to those of GFP transduced cells. Data are presented as mean fold change ±SD from 5 independent experiments, each in triplicate (*n* = 5; ****P* < 0.001). (c) Intracellular cystine levels were measured in *CTNS*^{-/-} ciPTEC after 24 hours from transient transfection with TFEB-GFP or TFEB(S142A)-GFP plasmids, corrected for protein concentrations, and normalized to those of GFP transfected cells. Data are presented as mean fold change ±SD from 3 independent experiments, each in triplicate (*n* = 3; **P* < 0.05; ****P* < 0.001). (d) Activities of the lysosomal enzyme β-hexosaminidase were determined in both culture media and in cell extracts from GFP and TFEB-GFP transduced *CTNS*^{-/-} ciPTEC. The histogram shows released enzyme activities measured as percentage of total activities and expressed as fold change. Data are presented as mean ±SD from 3 independent experiments, each in quintuplicate (*n* = 3; **P* < 0.05). (e) Extracellular cystine levels were measured in the medium of *CTNS*^{-/-} ciPTEC after 24 hours from transient transfection with GFP or TFEB-GFP plasmids. Data are presented as mean fold change ±SD from 3 independent experiments, each in triplicate (*n* = 3; **P* < 0.05).

significantly reduced (~1.5-fold of reduction in both the number and size of LAMP1 positive structures) (Figure 5d–f). No statistically significant differences were observed between untransfected or GFP transfected cystinotic ciPTEC cells (Figure 5b, c, e, and f).

These data indicate that TFEB overexpression completely rescues the studied morphological abnormalities of the lysosomal compartment observed in *CTNS*^{-/-} ciPTEC.

Nuclear versus cytoplasmic distribution of TFEB correlates with the status of lysosomal compartment in *CTNS*^{-/-} cells

Fluorescence analysis performed in *CTNS*^{-/-} ciPTEC transduced cells, revealed a predominantly cytosolic distribution of TFEB (Supplementary Figure S2A). Due to the apparent discrepancy

with the data obtained from transient transfections, in which TFEB was mainly localized into the nucleus of *CTNS*^{-/-} cells (Figure 2b), we reasoned that the main difference between the 2 experimental conditions was the duration of overexpression of TFEB. Cells transfected with TFEB-GFP plasmids were analyzed after 24 hours from transfection, whereas cells transduced with the lentiviral vectors were analyzed after more than 1 month from transduction. We therefore performed a time-course of TFEB-GFP overexpression to investigate both its nuclear/cytoplasmic distribution and the morphology of the lysosomal compartment. After 24 hours from transient transfection, TFEB-GFP was mostly localized in the nucleus of *CTNS*^{-/-} ciPTEC as shown in Figure 6a. The lysosomal compartment in these TFEB-GFP overexpressing cells was

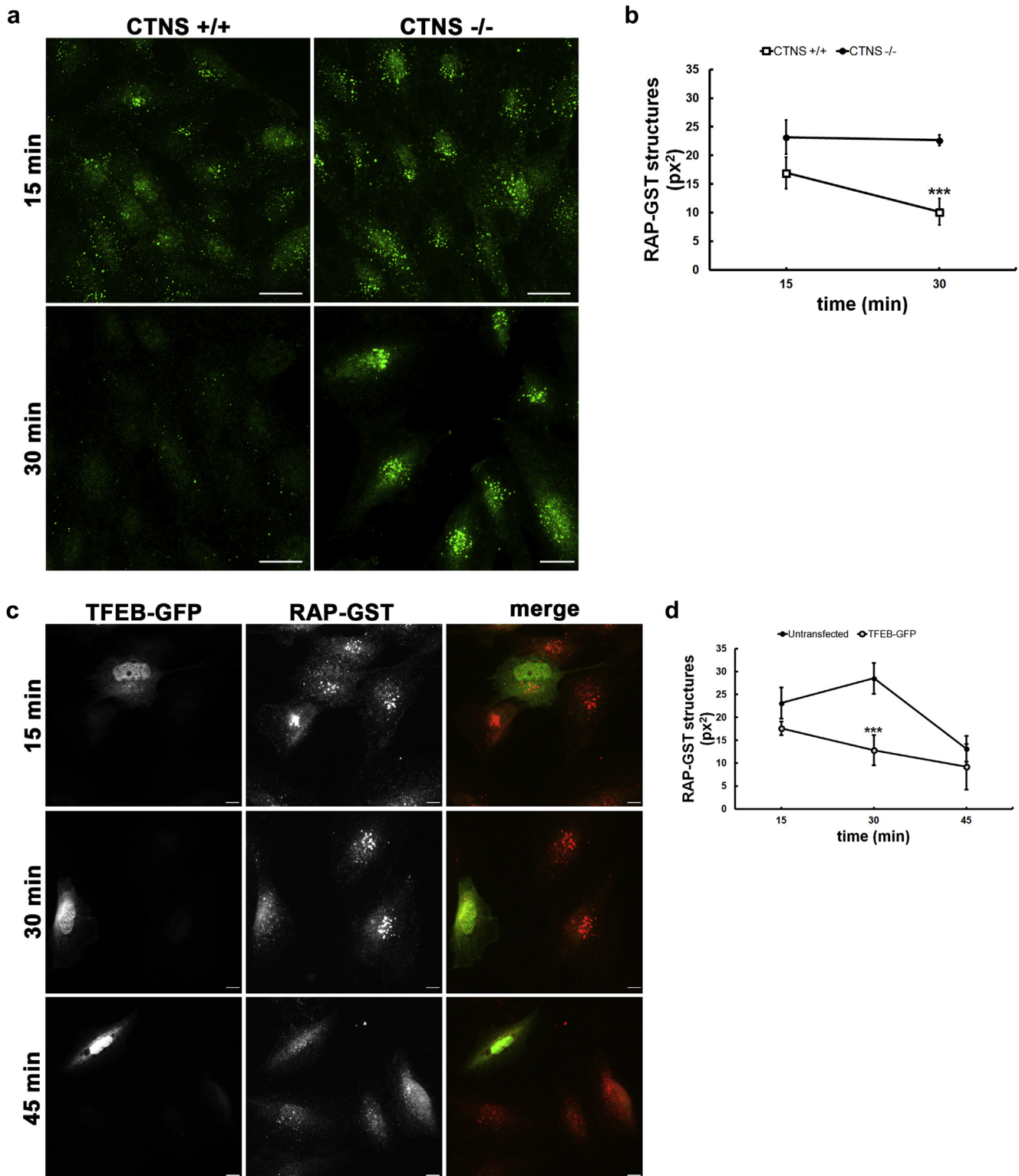


Figure 4 | TFEB overexpression stimulates RAP-GST cargo processing in cystinotic cells. (a) Representative fluorescence images from *CTNS*^{+/+} and *CTNS*^{-/-} conditionally immortalized proximal tubular epithelial cells stained with anti-glutathione-S-transferase (GST) antibodies (green) after 15 and 30 minutes from receptor-associated protein (RAP)-GST internalization. Bar = 25 μ m. (b) The size of RAP-GST positive structures (px²) was measured in both *CTNS*^{+/+} and *CTNS*^{-/-} conditionally immortalized proximal tubular epithelial cells after 15 and 30 minutes from the shift to 37 °C. Data are presented as the mean size of RAP-GST structures expressed in px² ($n = 3$; *** $P < 0.001$). (c) Representative fluorescence images from *CTNS*^{-/-} conditionally immortalized proximal tubular epithelial cells transfected with transcription factor EB (TFEB)-green fluorescent protein (GFP) plasmid for 24 hours (green) and stained with anti-GST antibodies (red) after 15, 30, and 45 minutes from RAP-GST internalization. Bar = 10 μ m. (d) The size of RAP-GST positive structures (px²) was measured in both TFEB-GFP transfected or adjacent untransfected cells after 15, 30, and 45 minutes from the shift to 37 °C. Data are presented as the mean size of RAP-GST structures expressed in px² ($n = 3$; *** $P < 0.001$).

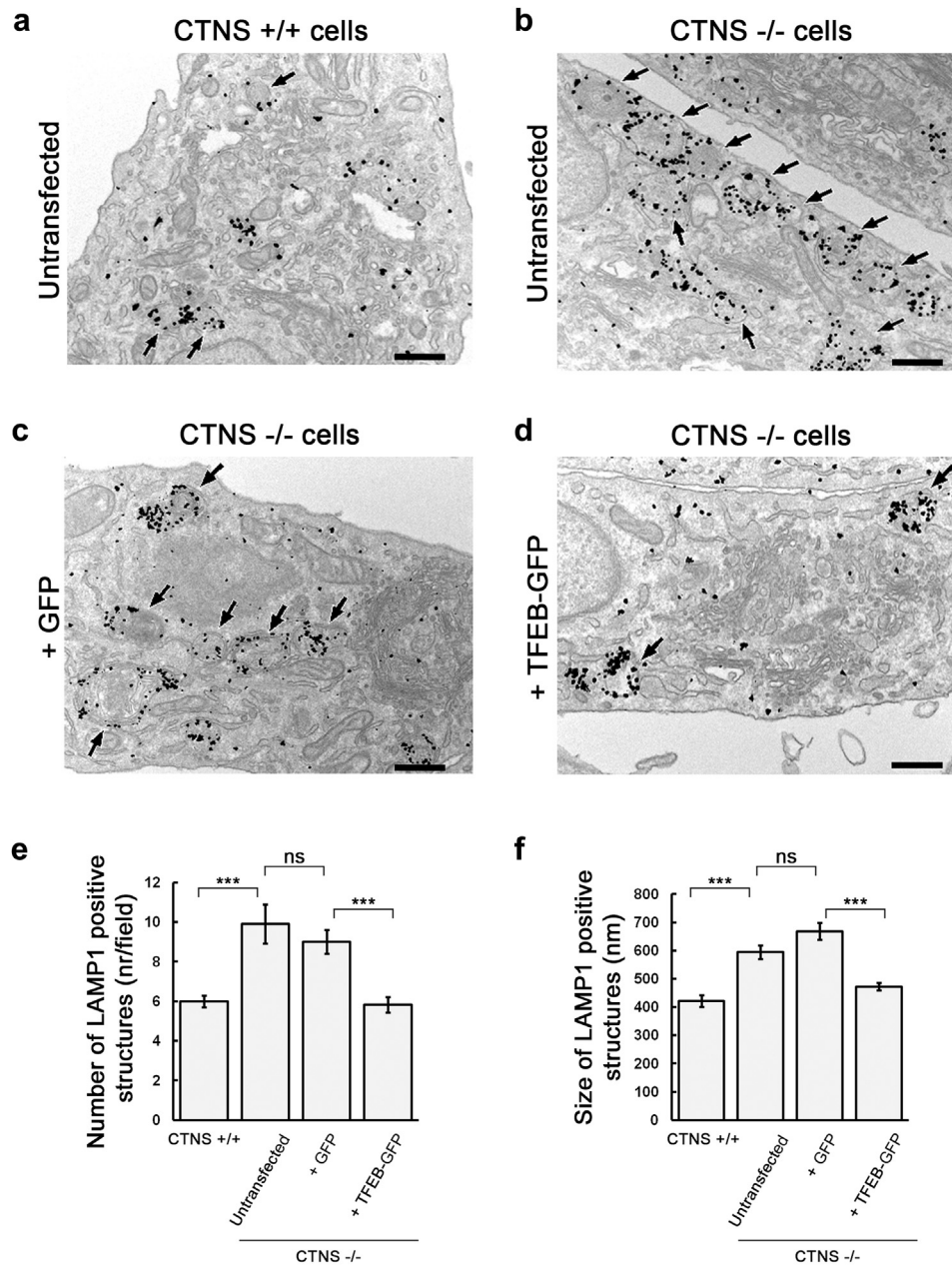


Figure 5 | TFEB overexpression reduces both the number and the size of lysosomes in cystinotic cells. (a,b) Representative electron micrographs from *CTNS*^{+/+} and *CTNS*^{-/-} conditionally immortalized proximal tubular epithelial cells labeled with anti-LAMP1 antibodies and prepared for immuno-electron microscopy. (c,d) Representative electron micrographs from *CTNS*^{-/-} conditionally immortalized proximal tubular epithelial cells transduced with lentivirus for control green fluorescent protein (GFP) or transcription factor EB (TFEB)-GFP expression and sorted by fluorescence-activated cell sorter as described in the materials and methods. LAMP1 positive structures are indicated by arrows. Bar = 500 nm. (e) Morphometric analysis was done from electron microscopy images acquired from thin sections using the same magnification. The number of LAMP1 positive structures was counted within 36 μm^2 fields of view and expressed as mean \pm SEM. (f) The size of LAMP1 positive structures was measured (100 structures for each experimental condition) and expressed as mean \pm SEM. (****P* < 0.001; ns, not statistically significant).

morphologically unaffected when compared with untransfected *CTNS*^{-/-} ciPTEC. Indeed, we did not observe any significant difference in size between lysosomes of untransfected or TFEB-GFP *CTNS*^{-/-} ciPTEC (Figure 6a, Supplementary Figure 2B). However, after 1 week (168 hours) from transient transfection, the morphology of lysosomes in TFEB-GFP *CTNS*^{-/-} transfected cells changed. TFEB-GFP *CTNS*^{-/-}

ciPTEC showed reduced size of lysosomes, as compared to adjacent untransfected cells and TFEB-GFP distribution became predominantly cytosolic (Figure 6a). Conversely, control GFP transient transfection did not affect lysosomal compartment in cystinotic ciPTEC after 168 hours (Supplementary Figure S2C). These observations were confirmed and quantified by high-content imaging. In this

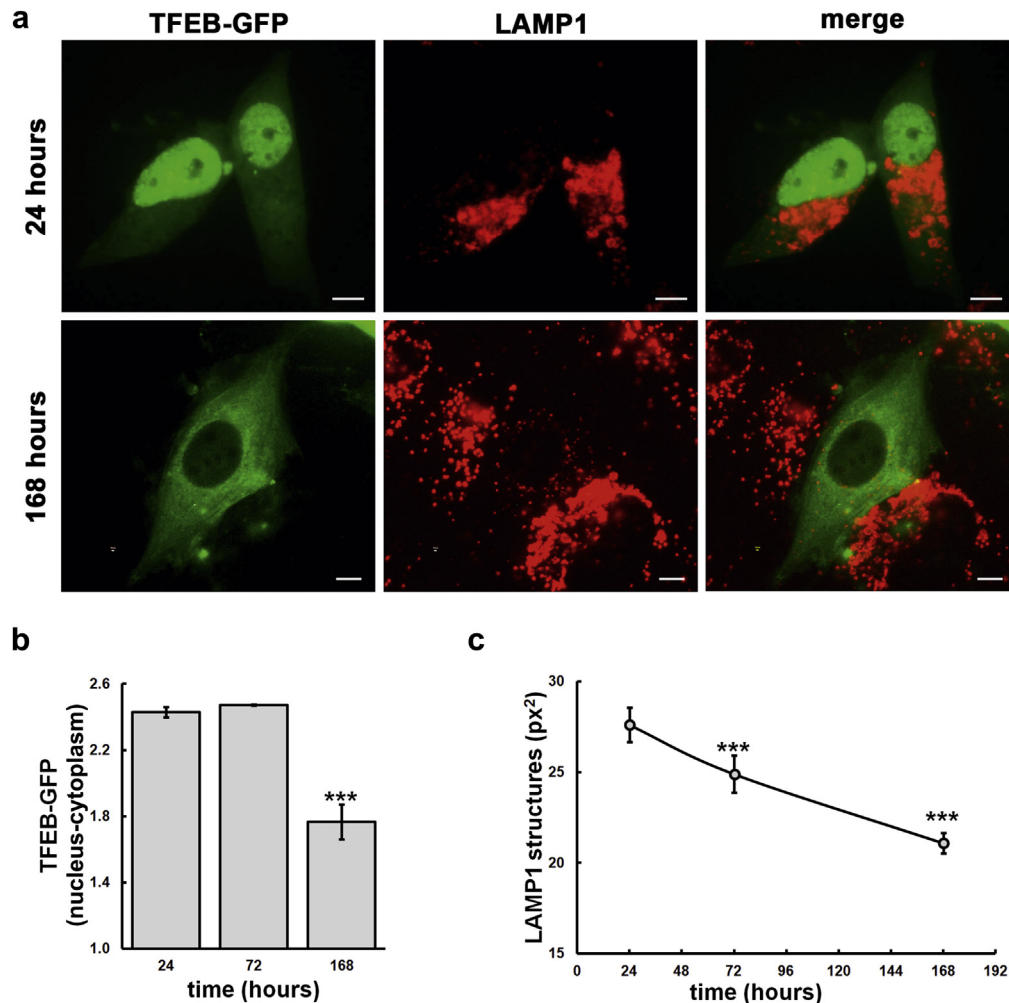


Figure 6 | Time course of TFEB-GFP overexpression. (a) Representative fluorescence images from *CTNS*^{-/-} conditionally immortalized proximal tubular epithelial cells transfected with transcription factor EB (TFEB)–green fluorescent protein (GFP) plasmid (green) and stained with anti-LAMP1 antibodies (red) after 24 and 168 hours from transfection. Bar = 10 μm . (b) TFEB nucleus-cytoplasm ratio was analyzed in *CTNS*^{-/-} conditionally immortalized proximal tubular epithelial cells after 24, 72, and 168 hours from transfection with TFEB-GFP plasmid. Data are presented as the ratio value resulting from the average intensity of nuclear TFEB-GFP fluorescence divided by the average of the cytosolic intensity of TFEB-GFP fluorescence. (c) The size of LAMP1 positive structures (px^2) was measured in TFEB-GFP *CTNS*^{-/-} conditionally immortalized proximal tubular epithelial cells after 24, 72, and 168 hours from transient transfection. Data are presented as the mean value of lysosomal size expressed in px^2 (***) $P < 0.001$).

assay, we analyzed both the distribution of TFEB and the size of the lysosomes in *CTNS*^{-/-} ciPTEC after different time points from TFEB-GFP transient transfection (24, 72, and 168 hours). After 24 and 72 hours from transient transfection, TFEB-GFP was mainly localized in the nucleus of cystinotic ciPTEC (~ 2.4 of TFEB-GFP nucleus-cytoplasm ratio in both experimental conditions) (Figure 6b). Seventy-two hours of TFEB-GFP transient transfection only induced a slight reduction of lysosomal size in cystinotic ciPTEC (mean size of $27.6 \pm 0.9 \text{ px}^2$ and $24.9 \pm 1 \text{ px}^2$, after 24 and 72 hours from transient transfection, respectively) (Figure 6c). However, after 168 hours from TFEB-GFP transient transfection, the size of lysosomes in cystinotic cells was drastically changed (mean size of $21.1 \pm 0.6 \text{ px}^2$) (Figure 6c). At this same time point, the TFEB nuclear-cytoplasmic ratio was markedly reduced (~ 1.8) (Figure 6b).

Collectively, these data suggest that nuclear localization of TFEB-GFP after short expression reflects lysosome stress in *CTNS*^{-/-} cells. Prolonged expression of TFEB allows cells to overcome, at least in part, such stress and to balance lysosome homeostasis through clearance of cystine-loaded lysosomes. Consequently, TFEB returns to the cytosol.

DISCUSSION

There are two important observations we made in this study. First, we found that the absence of cystinosis decreases TFEB level. Second, we demonstrated that genetic and chemical activation of TFEB produces a reduction of cystine accumulation and a stimulation of delayed cargo processing and rescues the abnormalities of the morphology of the lysosomal compartment in cystinotic cells.

TFEB is a master regulator of the coordinated lysosomal expression and regulation network. TFEB specifically recognizes and binds the coordinated lysosomal expression and regulation–box sequence present in the regulatory region of many lysosomal genes, leading to activation of their expression.¹⁹ A coordinated lysosomal expression and regulation–box has been identified in the promoter of *CTNS* gene.²⁴ Accordingly we confirmed that overexpression of TFEB strongly increases expression of *CTNS* mRNA in different cell lines (data not shown). Johnson *et al.*¹² have recently proposed that down-regulation of Rab27a expression in cystinosis is caused by TFEB dysfunction. This hypothesis was supported by the finding of 3 possible TFEB-mediated regulatory elements in the promoter regions of the mouse and human Rab27a genes.²⁵ Here we found that cystinotic cells have decreased levels of TFEB, which appears to be related to cystinosin deficiency *per se* and not to cystine accumulation. Treating cystinotic cells with the cystine-depleting agent, cysteamine, indeed did not rescue this defect, whereas knocking down the expression of *CTNS* led to significant reduction of TFEB expression and only to a slight accumulation of intracellular cystine (compared with the levels of cystine accumulated in cystinotic cells; data not shown). Napolitano *et al.*¹⁰ also demonstrated that reduction of cystine by cysteamine treatment did not rescue defective chaperone-mediated autophagy both in cystinotic mouse fibroblasts and cystinotic mice. Moreover, a recent paper from Andrzejewska *et al.*²⁶ showed that cystinosin is a component of the mTOR complex 1 and has a direct role in the regulation of the activity of this complex. Indeed, cysteamine treatments had no effects on impaired mTOR signaling in *CTNS*^{-/-} cells. All together, these data strongly support the hypothesis that cystinosin has additional roles to its cystine transporting activity and, directly or indirectly, contributes to the modulation of TFEB intracellular expression and activity. However, further studies are required to clarify the mechanisms linking *CTNS* and TFEB expression.

As mentioned, Andrzejewska *et al.*²⁶ demonstrated that mTOR signaling is altered in cystinotic cells. Moreover, lack of cystinosin and accumulation of cystine cause high lysosomal stress that results in abnormal morphology of the lysosomal compartment, characterized by enlarged lysosomes.¹³ Both mTOR dysregulation and lysosomal stress induce TFEB activation and nuclear translocation.²⁷ Consistently, we highlighted TFEB nuclear translocation in cystinotic cells. By analogy of what has been observed in other LSDs, we could demonstrate by both a chemical and genetic approach, that TFEB stimulation can reduce cystine levels in cystinotic cells, promoting lysosomal exocytosis. Johnson *et al.*¹² also demonstrated that up-regulation of the exocytic pathway by overexpression of the constitutively active form of Rab27a decreases cystine content in cystinotic cells. However, we cannot exclude that other pathways, such as autophagy, can contribute to TFEB-induced cellular clearance. Many studies demonstrated that genetic and/or chemical activation of TFEB promotes autophagic

clearance of aberrant aggregates.^{21,22,28} In this context, it is important to note that recent advances in the field of cystinosis have highlighted that aberrant autophagy is an important contributor to the pathogenesis of the disease.^{10,29}

The discovery of compounds, such as genistein²³ and 2-hydroxypropyl- β -cyclodextrin,³⁰ able to stimulate endogenous TFEB activity has provided an attractive alternative to gene-transfer therapy in the treatments of diseases that potentially can benefit from TFEB activation. Genistein, a natural isoflavone present in soy, has been proposed as therapeutic agent for the LSD, mucopolysaccharidosis, for its ability to inhibit the synthesis and reduce lysosomal storage of glycosaminoglycans³¹ and, recently, for its ability to activate TFEB.^{23,32} Moreover genistein and soy products have gained attention for their pleiotropic effects and have been suggested to mitigate many conditions such as obesity, metabolic syndrome, and cancer. In this contest, cystinotic patients could potentially benefit from increased genistein intake in their diet or from genistein supplementation also for its antioxidant and anti-inflammatory properties.^{33,34} Indeed, cystinosis has been also characterized by enhanced oxidative stress³⁵ and inflammation.³⁶ Because genistein is able to regulate different cellular pathways, we checked the impact of this treatment on chaperone-mediated autophagy, but no ameliorations of this phenotype were highlighted in cystinotic cells (Supplementary Figure S3A and B).

Overexpression of exogenous TFEB was able to reduce cystine levels after 24 hours from transient transfection, indicating a rapid effect on mobilization of cystine deposits. Moreover, we demonstrated that cystinotic cells overexpressing TFEB show faster processing of endocytic cargo if compared with untransfected cells (Figure 4c and d). This consequence of TFEB overexpression opens new insights in the role of this protein but, most importantly, suggests that TFEB activation can also improve renal Fanconi syndrome in cystinosis. On the contrary, the abnormalities of the lysosomal compartment were not rescued after 24 hours. Recently, Ivanova *et al.*¹³ also demonstrated that treatment with the cystine-depleting agent, cysteamine, was not efficient in restoring lysosomal morphology within 24 hours in *CTNS*-depleted cells. Thus, we wondered whether the complete rescue of lysosomal function would require treatment longer than 24 hours. After a week from transient transfection, the lysosomal compartment in cystinotic cells overexpressing TFEB was significantly modified and became comparable to that of control cells. As a result, TFEB no longer accumulated into the nucleus of cystinotic cells. These results support the hypothesis that depletion of cystine *per se* does not rescue all cystinotic phenotypes.¹⁰ TFEB being a transcription factor, it is likely that stimulation and/or suppression of other cellular pathways could be responsible for the rescue of these additional cystinotic cell phenotypes. This strongly suggests that other treatments complementary to current therapies aimed at decreasing lysosomal overload are needed.

MATERIALS AND METHODS

Cell culture and treatments

Human kidney-2 cells (American Type Culture Collection CRL-2190) were grown in Dulbecco's modified Eagle's medium-F12 (Invitrogen, Life Technologies, Camarillo, CA) supplemented with 5% fetal bovine serum, 100 units/ml penicillin and 100 µg/ml streptomycin, 10 µg/ml insulin from bovine pancreas, 5.5 µg/ml human transferrin, and 5 ng/ml sodium selenite. HepG2 cells (American Type Culture Collection) were cultured in Dulbecco's modified Eagle's medium supplemented with 10% fetal bovine serum, 2 mM L-glutamine, 100 units/ml penicillin, and 100 µg/ml streptomycin. ciPTEC were kindly provided by Dr. Elena N. Levchenko and cultured as described in Wilmer *et al.*³⁷ Human cystinotic fibroblasts were kindly provided by the Cell Lines and DNA Bank of Patients Affected by Genetic Diseases (Laboratorio di Diagnosi Pre e Postnatale delle Malattie Metaboliche, Istituto G. Gaslini, Italy, partially supported by the Telethon Foundation). Fibroblasts were grown in Dulbecco's modified Eagle's medium supplemented with 10% fetal bovine serum, 1 mM sodium pyruvate (Invitrogen), 2 mM L-glutamine, 100 units/ml penicillin, and 100 µg/ml streptomycin. Cells were grown in a humidified atmosphere with 5% CO₂ at 37 °C. Unless otherwise specified, all reagents were purchased from Sigma-Aldrich (St. Louis, MO). After 24 hours from splitting in 24-well plates, cells were incubated with fresh nonsupplemented medium containing DMSO at a final concentration of 0.1%, or genistein at a final concentration of 100 µM, 0.1% DMSO for 24 hours.

Plasmid and siRNA transfection

TFEB-GFP plasmid was generated by Dr. Annelies Michiels (Viral Vector Core, Leuven, Belgium). ciPTEC cells were transfected with plasmids by Lipofectamine LTX and Plus Reagent (Invitrogen) according to the manufacturer's instructions. Mutant TFEB(S142A)-GFP was generated by the Q5-Site directed mutagenesis kit (New England, BioLabs Inc., Ipswich, MA) according to the manufacturer's instructions. Human kidney-2 and HepG2 cells were transfected with siGENOME human CTNS or TFEB siRNA, SMART pool (Dharmacon, Thermo Scientific, Dublin, Ireland) by Lipofectamine Reagent (Invitrogen) according to the manufacturer's instructions.

Lentivirus transduction

Lentivirus expressing GFP and TFEB-GFP were prepared, amplified, and purified by Dr. Annelies Michiels. Lentivirus transduction was performed as described in supplementary experimental procedures.

RNA extraction and quantitative real-time PCR

Total RNA was extracted by TRIzol reagent (Ambion, Life Technologies, Foster, CA) and cDNA was synthesized using the EuroScript RT-PCR kit (EuroClone, Milano, Italy) according to the manufacturer's instructions. Quantitative PCR assays (shown in Figure 1) were performed using SensiMix II Probe Hi-ROX kit (Bioline, London, UK) and the gene-expression assays for human TFEB and CTNS (Applied Biosystem, Foster, CA). Quantitative PCR assays from genistein untreated or treated cells (Supplementary Figure S1D) were performed by SYBR FAST quantitative PCR Kit Master Mix (Kapa Biosystems, Wilmington, MA) with corresponding primers listed in Supplementary Table S1. Gene expression data were determined using the 2^{-Δct} method and normalized using human glyceraldehyde-3-phosphate dehydrogenase.

Western blot

For total cell extracts, cells were lysed in radioimmunoprecipitation assay buffer, sonicated, and centrifuged for 10 minutes at 13,000 rpm at 4 °C. Alternatively, nuclear and cytosolic fractions were obtained as described in Martina and Puertollano.³⁸ Protein concentrations were measured using the Bio-Rad Protein Assay (Bio-Rad Laboratories, Inc., Hercules, CA). Proteins were separated by 12% sodium dodecylsulfate-polyacrylamide gel electrophoresis and immunoblotted onto a nitrocellulose membrane (Whatman Bioscience Ltd., Maidstone, UK). The membrane was blocked with 5% bovine serum albumin in Tris-buffered saline, 0.1% Tween 20 and incubated with primary antibodies anti-Actin (Ambion), anticystinosis (Abnova, Taipei City, Taiwan), anti-glyceraldehyde-3-phosphate dehydrogenase, anti-TFEB, or antihistone H3 (Cell Signaling, Danvers, MA), and with horseradish peroxidase secondary antibody conjugate IgG (Santa Cruz Biotechnology, Inc., Santa Cruz, CA). Immunoblots were developed with LiteAblot EXTEND (EuroClone, Milan, Italy) and acquired with the ChemiDoc XRS System (Bio-Rad).

Measurement of extracellular and intracellular cystine levels

To measure extracellular cystine levels, cells were cultured in cystine-free medium for 24 hours. Extracellular and intracellular cystine levels were measured as previously reported.³⁹

β-Hexosaminidase activity assay

β-Hexosaminidase activity was measured in both cell extract and medium as described previously.⁴⁰

Endocytosis assay

RAP-GST processing was assessed as previously described by Ivanova *et al.*¹³ RAP-GST ligand and anti-GST antibodies were kindly provided by Dr. Maria Antonietta De Matteis.

Immuno-electron microscopy

Cells for pre-embedding immuno-EM were fixed, permeabilized, and labeled as described previously.⁴¹ Antihuman LAMP1 (clone H4A3) antibodies were purchased by Developmental Studies Hybridoma Bank (Iowa City, IA). From each sample, thin 65 nm sections were cut using a Leica EM UC7 ultramicrotome (Wetzlar, Germany). EM images were acquired from thin sections using a FEI Tecnai-12 electron microscope (FEI, Eindhoven, Netherlands) equipped with a VELETTA CCD digital camera (Soft Imaging System GmbH, Münster, Germany). Morphometric analysis of number and size of LAMP1 positive structures was performed using iTEM software (Olympus SYS, Isee, Germany). Number of lysosomes was counted using the same magnification within 36 µm² fields of view.

For measurement of the lysosome diameter, the stereology approach (sequential random sampling methods) was used. Lysosome diameters were estimated on EM images. EM images were treated as vertical sections. The diameters were obtained using the point sampled intercepts method (see Gundersen *et al.*⁴²).

Fluorescence assays

Untransfected or transfected cells were grown on glass coverslips, fixed with 4% paraformaldehyde and permeabilized with phosphate-buffered saline containing 0.05% saponin, 0.5% bovine serum albumin, 50 mM NH₄Cl and incubated with anti-LAMP1 antibody (Santa Cruz Biotechnology, Inc., Santa Cruz, CA). Nuclei were stained by Hoechst 33342, trihydrochloride, trihydrate (Invitrogen). Images were acquired on a Nikon Eclipse E600 microscope (Nikon Instruments, Melville, NY) equipped with epifluorescence optics and

processed with ImageJ software (National Institute of Health, Bethesda, MD).

For the time-course experiments, *CTNS*^{-/-} ciPTEC were cultured in 12-well plates and transfected with TFEB-GFP plasmid as described herein. After 8 hours from transient transfection, cells were trypsinized and seeded on 96-well plates and fixed after 24, 72, and 168 hours from transient transfection. After fixing, cells were permeabilized and labeled as described. For the analysis, 10 images per each well of the 96-well plate were acquired by using automated microscopy (Operetta High Content Imaging System; PerkinElmer, Waltham, MA). TFEB localization was analyzed by a dedicated script calculating the ratio value resulting from the average intensity of nuclear TFEB-GFP fluorescence divided by the average of the cytosolic intensity of TFEB-GFP fluorescence. Lysosomal area was analyzed in TFEB-GFP cells by performing LAMP1 staining. All the scripts for the analysis were developed on Harmony software (PerkinElmer).

DISCLOSURES

All the authors declared no competing interests.

ACKNOWLEDGMENTS

The authors thank Dr. Gianna Di Giovamberardino, Dr. Alessia Palma, and Dr. Ezio Giorda for technical support and Professor Olivier Devuyt and Dr. Alessandro Luciani for helpful discussions. They also thank Dr. Pierre Courtoy for critical reading of the manuscript. These studies were supported by a grant from the Cystinosis Research Foundation, USA.

SUPPLEMENTARY MATERIAL

Supplementary Results

Figure S1. (A) Intracellular cystine levels were measured in *CTNS*^{-/-} conditionally immortalized proximal tubular epithelial cells, untreated or treated with 100 μM cysteamine for 24 hours. Data are presented as mean fold change ± SD (*n* = 5; *** *P* < 0.001). (B) Transcription factor EB (TFEB) mRNA and (C) *CTNS* mRNA levels were analyzed in HepG2 cells after 96 hours from transfection with nontargeting (CTRL) or *CTNS* small, interfering RNAs (*CTNS* knock down). Glyceraldehyde-3-phosphate dehydrogenase was used as reference. Data are presented as mean fold change ± SEM from 3 independent experiments, each in triplicate (*n* = 3; **P* < 0.05; ****P* < 0.001). (D) Relative mRNA expression levels of representative coordinated lysosomal expression and regulation coordinated lysosomal expression and regulation network genes in *CTNS*^{-/-} conditionally immortalized proximal tubular epithelial cells treated with genistein (100 μM) for 24 hours. *ASAH1*, *CTSD*, *SMPD1*, and *SQSTM1* mRNA expression levels were obtained by quantitative polymerase chain reaction, corrected for the expression of the housekeeping genes glyceraldehyde-3-phosphate dehydrogenase, and normalized to those of dimethyl sulfoxide (DMSO)-treated cells (black line). Data are reported as mean fold change ± SD from 3 independent experiments (*n* = 3; *P* < 0.05). (E) Intracellular cystine levels were measured in cystinotic fibroblasts after treatment with genistein (100 μM) for 24 hours, corrected for protein concentrations, and normalized to those of DMSO-treated cells. Data are presented as mean fold change ± SD from 3 independent experiments, each in triplicate (*n* = 3; ****P* < 0.001). (F) The histogram shows the percentages of green fluorescent protein (GFP) or TFEB-GFP propidium iodide positive *CTNS*^{-/-} conditionally immortalized proximal tubular epithelial cells (24 hours of transfection). Data are presented as mean values ± SD from 3 independent experiments, each in triplicate (*n* = 3; ns = not statistically significant).

Figure S2. (A) Representative image of *CTNS*^{-/-} conditionally immortalized proximal tubular epithelial cells after transduction with

transcription factor EB (TFEB)–green fluorescent protein (GFP) (green) lentivirus and fluorescence-activated cell sorting. Bar = 100 μm.

(B) Representative image of LAMP1 (green) staining in control *CTNS*^{+/+} and cystinotic *CTNS*^{-/-} conditionally immortalized proximal tubular epithelial cells. Nuclei are blue. Bar = 10 μm. (C) Representative image of LAMP1 (red) staining in *CTNS*^{-/-} conditionally immortalized proximal tubular epithelial cells after 168 hours from transient transfection with control GFP plasmid (green). Bar = 10 μm.

Figure S3. (A) Representative immunoblot showing LAMP2a protein levels in *CTNS*^{+/+} and *CTNS*^{-/-} fibroblasts after treatment with dimethyl sulfoxide or genistein (100 μM) for 24 hours. LAMP2a levels were normalized for Actin levels. (B) The histogram shows relative LAMP2a levels expressed as mean fold change ± SD from 3 independent experiments (*n* = 3; ns = not statistically significant).

Table S1. List of the primer sequences used for quantitative real-time polymerase chain reaction experiments.

Supplementary material is linked to the online version of the paper at www.kidney-international.org.

REFERENCES

1. Emma F, Nesterova G, Langman C, et al. Nephropathic cystinosis: an international consensus document. *Nephrol Dial Transplant*. 2014;29(suppl 4):iv87–94.
2. Levtchenko E, van den Heuvel L, Emma F, Antignac C. Clinical utility gene card for: cystinosis. *Eur J Hum Genet*. 2014;22. <http://dx.doi.org/10.1038/ejhg.2013.204>.
3. Forestier L, Jean G, Attard M, et al. Molecular characterization of *CTNS* deletions in nephropathic cystinosis: development of a PCR-based detection assay. *Am J Hum Genet*. 1999;65:353–359.
4. Town M, Jean G, Cherqui S, et al. A novel gene encoding an integral membrane protein is mutated in nephropathic cystinosis. *Nat Genet*. 1998;18:319–324.
5. Kalatzis V, Cherqui S, Antignac C, Gasnier B. Cystinosis, the protein defective in cystinosis, is a H(+)-driven lysosomal cystine transporter. *EMBO J*. 2001;20:5940–5949.
6. Gahl WA, Thoene JG, Schneider JA. Cystinosis. *N Engl J Med*. 2002;347:111–121.
7. Park M, Helip-Wooley A, Thoene J. Lysosomal cystine storage augments apoptosis in cultured human fibroblasts and renal tubular epithelial cells. *J Am Soc Nephrol*. 2002;13:2878–2887.
8. Laube GF, Shah V, Stewart VC, et al. Glutathione depletion and increased apoptosis rate in human cystinotic proximal tubular cells. *Pediatr Nephrol*. 2006;21:503–509.
9. Sansanwal P, Sarwal MM. Abnormal mitochondrial autophagy in nephropathic cystinosis. *Autophagy*. 2010;6:971–973.
10. Napolitano G, Johnson JL, He J, et al. Impairment of chaperone-mediated autophagy leads to selective lysosomal degradation defects in the lysosomal storage disease cystinosis. *EMBO Mol Med*. 2015;7:158–174.
11. Sansanwal P, Yen B, Gahl WA, et al. Mitochondrial autophagy promotes cellular injury in nephropathic cystinosis. *J Am Soc Nephrol*. 2010;21:272–283.
12. Johnson JL, Napolitano G, Monfregola J, et al. Upregulation of the Rab27a-dependent trafficking and secretory mechanisms improves lysosomal transport, alleviates endoplasmic reticulum stress, and reduces lysosome overload in cystinosis. *Mol Cell Biol*. 2013;33:2950–2962.
13. Ivanova EA, De Leo MG, Van Den Heuvel L, et al. Endo-lysosomal dysfunction in human proximal tubular epithelial cells deficient for lysosomal cystine transporter cystinosis. *PLoS One*. 2015;10:e0120998.
14. Raggi C, Luciani A, Nevo N, et al. Dedifferentiation and aberrations of the endolysosomal compartment characterize the early stage of nephropathic cystinosis. *Hum Mol Genet*. 2014;23:2266–2278.
15. Gaide Chevronnay HP, Janssens V, Van Der Smissen P, et al. Time course of pathogenic and adaptation mechanisms in cystinotic mouse kidneys. *J Am Soc Nephrol*. 2014;25:1256–1269.
16. Thoene JG, Oshima RG, Crawhall JC, et al. Cystinosis: intracellular cystine depletion by aminothiols in vitro and in vivo. *J Clin Invest*. 1976;58:180–189.
17. Gahl WA, Reed GF, Thoene JG, et al. Cysteamine therapy for children with nephropathic cystinosis. *N Engl J Med*. 1987;316:971–977.

18. Settembre C, Fraldi A, Medina DL, Ballabio A. Signals from the lysosome: a control centre for cellular clearance and energy metabolism. *Nat Rev Mol Cell Biol.* 2013;14:283–296.
19. Sardiello M, Palmieri M, di Ronza A, et al. A gene network regulating lysosomal biogenesis and function. *Science.* 2009;325:473–477.
20. Medina DL, Fraldi A, Bouche V, et al. Transcriptional activation of lysosomal exocytosis promotes cellular clearance. *Dev Cell.* 2011;21:421–430.
21. Spampinato C, Feeney E, Li L, et al. Transcription factor EB (TFEB) is a new therapeutic target for Pompe disease. *EMBO Mol Med.* 2013;5:691–706.
22. Pastore N, Blomenkamp K, Annunziata F, et al. Gene transfer of master autophagy regulator TFEB results in clearance of toxic protein and correction of hepatic disease in alpha-1-anti-trypsin deficiency. *EMBO Mol Med.* 2013;5:397–412.
23. Moskot M, Montefusco S, Jakobkiewicz-Banecka J, et al. The phytoestrogen genistein modulates lysosomal metabolism and transcription factor EB (TFEB) activation. *J Biol Chem.* 2014;289:17054–17069.
24. Palmieri M, Impey S, Kang H, et al. Characterization of the CLEAR network reveals an integrated control of cellular clearance pathways. *Hum Mol Genet.* 2011;20:3852–3866.
25. Chiaverini C, Beuret L, Flori E, et al. Microphthalmia-associated transcription factor regulates RAB27A gene expression and controls melanosome transport. *J Biol Chem.* 2008;283:12635–12642.
26. Andrzejewska Z, Nevo N, Thomas L, et al. Cystinosis is a component of the vacuolar H⁺-ATPase-Ragulator-Rag complex controlling mammalian target of rapamycin complex 1 signaling [e-pub ahead of print]. *J Am Soc Nephrol.* pii: ASN.2014090937. Accessed 2015.
27. Settembre C, Zoncu R, Medina DL, et al. A lysosome-to-nucleus signalling mechanism senses and regulates the lysosome via mTOR and TFEB. *EMBO J.* 2012;31:1095–1108.
28. Kilpatrick K, Zeng Y, Hancock T, Segatori L. Genetic and chemical activation of TFEB mediates clearance of aggregated α -synuclein. *PLoS One.* 2015;10:e0120819.
29. Sansanwal P, Li L, Sarwal MM. Inhibition of intracellular clusterin attenuates cell death in nephropathic cystinosis. *J Am Soc Nephrol.* 2015;26:612–625.
30. Song W, Wang F, Lotfi P, et al. 2-Hydroxypropyl-beta-cyclodextrin promotes transcription factor EB-mediated activation of autophagy: implications for therapy. *J Biol Chem.* 2014;289:10211–10222.
31. Piotrowska E, Jakobkiewicz-Banecka J, Baranska S, et al. Genistein-mediated inhibition of glycosaminoglycan synthesis as a basis for gene expression-targeted isoflavone therapy for mucopolysaccharidoses. *Eur J Hum Genet.* 2006;14:846–852.
32. Moskot M, Jakobkiewicz-Banecka J, Kloska A, et al. Modulation of expression of genes involved in glycosaminoglycan metabolism and lysosome biogenesis by flavonoids. *Sci Rep.* 2015;5:9378.
33. Javanbakht MH, Sadria R, Djalali M, et al. Soy protein and genistein improves renal antioxidant status in experimental nephrotic syndrome. *Nefrologia.* 2014;34:483–490 [in English and Spanish].
34. Nagaraju GP, Zafar SF, El-Rayes BF. Pleiotropic effects of genistein in metabolic, inflammatory, and malignant diseases. *Nutr Rev.* 2013;71:562–572.
35. Vaisbich MH, Pache de Faria Guimaraes L, Shimizu MH, Seguro AC. Oxidative stress in cystinosis patients. *Nephron Extra.* 2011;1:73–77.
36. Prencipe G, Caiello I, Cherqui S, et al. Inflammation activation by cystine crystals: implications for the pathogenesis of cystinosis. *J Am Soc Nephrol.* 2014;25:1163–1169.
37. Wilmer MJ, Saleem MA, Masereeuw R, et al. Novel conditionally immortalized human proximal tubule cell line expressing functional influx and efflux transporters. *Cell Tissue Res.* 2010;339:449–457.
38. Martina JA, Puertollano R. Rag GTPases mediate amino acid-dependent recruitment of TFEB and MITF to lysosomes. *J Cell Biol.* 2013;200:475–491.
39. Pastore A, Massoud R, Motti C, et al. Fully automated assay for total homocysteine, cysteine, cysteinylglycine, glutathione, cysteamine, and 2-mercaptopyruvonylglycine in plasma and urine. *Clin Chem.* 1998;44:825–832.
40. Rodriguez A, Webster P, Ortego J, Andrews NW. Lysosomes behave as Ca²⁺-regulated exocytic vesicles in fibroblasts and epithelial cells. *J Cell Biol.* 1997;137:93–104.
41. Polishchuk EV, Concilli M, Iacobacci S, et al. Wilson disease protein ATP7B utilizes lysosomal exocytosis to maintain copper homeostasis. *Dev Cell.* 2014;29:686–700.
42. Gundersen HJ, Bendtsen TF, Korbo L, et al. Some new, simple and efficient stereological methods and their use in pathological research and diagnosis. *APMIS.* 1988;96:379–394.